Local Current Flow and Dissipation in Multi-filamentary YBCO Coated Conductor under the Influence of Microstructural Inhomogeneity

Zulkifli, Zulistiana
Department of Electrical and Electronic Systems Engineering, Graduate School of Information Science and Electrical Engineering, Kyushu University : Graduate Student

Fujiwara, Takashi
Department of Electrical and Electronic Systems Engineering, Graduate School of Information Science and Electrical Engineering, Kyushu University : Graduate Student

Nakamura, Tomoya
Department of Electrical and Electronic Systems Engineering, Graduate School of Information Science and Electrical Engineering, Kyushu University : Graduate Student

Kiss, Takanobu
Department of Electrical and Electronic Systems Engineering, Faculty of Information Science and Electrical Engineering, Kyushu University

他

https://doi.org/10.15017/1517813

出版情報：九州大学大学院システム情報科学紀要. 12 (1), pp.27-31, 2007-03-26. Faculty of Information Science and Electrical Engineering, Kyushu University
バージョン：

九州大学大学院
システム情報科学紀要
第12巻 第1号 平成19年3月

Research Reports on Information Science and
Electrical Engineering of Kyushu University
Vol.12, No.1, March 2007

Local Current Flow and Dissipation in Multi-filamentary YBCO Coated Conductor under the Influence of Microstructural Inhomogeneity

Zulistiana ZULKIFLI*, Takashi FUJIWARA*, Tomoya NAKAMURA*, Takanobu KISS**, Keiji ENPUKU***, Tomonori WATANABE†, Naoji KASHIMA†, Masami MORI†, Shigeo NAGAYA†, Akira IBI††, Yutaka YAMADA†† and Yuh SHIOHARA††

(Received December 15, 2006)

Abstract: Local current flow and dissipation in a three parallel 100μm-wide filamentary YBCO tape had been studied in order to investigate the current carrying capability in each filament under the influence of local obstacles. Structural inhomogeneity and local flux flow dissipation have been visualized by using thermal laser stimulation technique and its local current density was measured by scanning SQUID microscope. By combining local current distribution with dissipation, we made estimations on local the J_c and I_c values in each filament. Results have shown a current imbalance on the current sharing in the filamentary structure. It has been shown that the I_c is possibly influenced significantly if the filament size reaches 100μm scale because of current blocking obstacles.

Keywords: Filamentary structure, Supercurrent flow, Flux flow dissipation, Current carrying capability, Microstructural inhomogeneity

1. Introduction

The second-generation high temperature superconducting (HTS) wire is based on coated conductor technology, where a textured $YBa_2Cu_3O_{7-\delta}$ (YBCO) film is deposited on a buffered flexible metal substrate. The HTS coated conductor (CC) however, has not been optimized for ac applications such as motors, generators, and transformers. The current CC dimensions will make the superconducting layer to be exposed to time varying magnetic field, and due to the irreversible flux movement, it will generate large hysteretic losses in perpendicular field which is proportionate to the width of the CC.

In order to minimize ac hysteretic losses, Carr and Oberly [1] proposed subdividing the HTS layer into micro-filamentary structure to reduce the CC width. However, this design also makes it susceptible to local obstacles that may influence its current carrying capability in multi-filaments when the size becomes several 100μm length scale. Our previous results using low temperature scanning laser microcopy (LTSLM) showed that local defects in YBCO single tape induce localized dissipation that range from several tens of μm to few hundred μm [2].

The critical current I_c information is very crucial in investigating the current carrying capability and if the filaments' I_c is not uniform, current flow in each filament becomes inhomogeneous and may cause instability. This results in the increase of ac loss in each filament. The I_c value is usually defined at the mean electric field $E_c = 1\mu$V/cm and also by assuming a uniform current density in the macroscopic cross-sectional area of the sample. However, reports have shown that local $E(x, y)$ can vary by several orders of magnitude due to current redistribution around macroscopic defects. Therefore, to truly understand what controls I_c, it is important to correlate the local E distribution with structural inhomogeneities [3].

If the filament size is large enough, we may attach voltage terminals as well as current terminals directly to each filaments, and investigate its current carrying property by four-point-probe method. However, it is hardly possible to measure each filament by the conventional method when the scale becomes around the size of 100μm. We cannot separately bias each filament, and measure voltages in each filament neither. Therefore, we have developed spatially resolved measurement techniques that al-

* Department of Electrical and Electronic Systems Engineering, Graduate Student
** Department of Electrical and Electronic Systems Engineering
*** Department of Superconductivity
† Chubu Electric Power Co.
†† Superconductivity Research Laboratory, International Superconductivity Technology Center

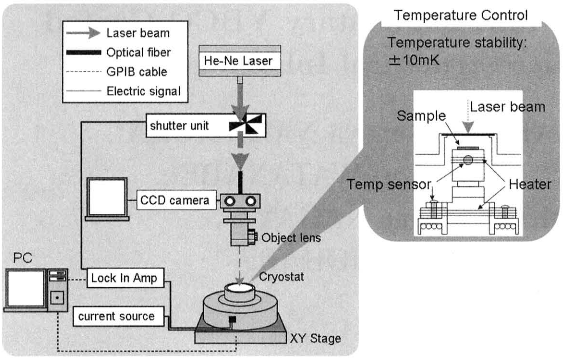

Fig. 1　Setup for the thermal laser stimulation imaging.

low us to measure local dissipation and current flow complementarily in μm length scale. In this paper, we investigate current carrying capability in each filament under the influence of local obstacles by applying the novel techniques.

2. Principle of Measurements

Mapping of the current distribution in the HTS layer has been accomplished by a variety of methods including magneto-optical imaging [4], scanning Hall probe [5], and hot spot scanning techniques such as low temperature scanning electron microscopy (LT-SEM) [6] and low temperature scanning laser microscopy (LTSLM) [2),3]. In this study we use thermal laser stimulation techniques such as Seebeck Effect Imaging (SEI) and LTSLM so as to visualize local defects and dissipation under superconducting state, respectively. We also visualized the local current flow in the filamentary structure by using Scanning SQUID Microscope (SSM).

Figure 1 is the setup for the thermal laser stimulation imaging technique. We used He-Ne laser to irradiate the sample surface and the voltage signal is measured by using lock-in technique [7]. At room temperature (RT) the irradiation of the laser will induce Seebeck voltage, $\nabla\phi$. In this study, we visualize defects by the SEI. Namely, we measured thermally induced transverse voltage V_x at each laser irradiation spot, $V_x = (S_{ab} - S_x)\delta T$ where V_x represents the in-plane defects; S_{ab} and S_x are the Seebeck constants at ab-plane and defect direction; δT is the temperature difference due to local heating by the laser beam.

Local dissipation in a superconducting state has been visualised by the LTSLM. By performing the experiment at superconducting temperature (ST), the laser modulated local temperature thus induced a modulation of the J_c locally when the multi-filaments is subjected to a dc bias current, I_b. The

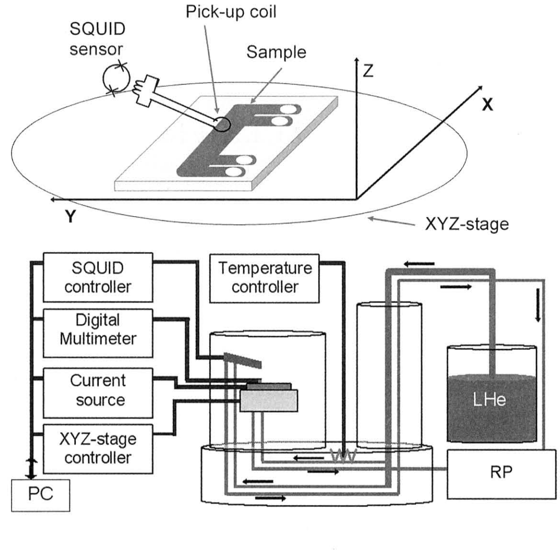

Fig. 2　Schematic diagram of scanning SQUID microscope system.

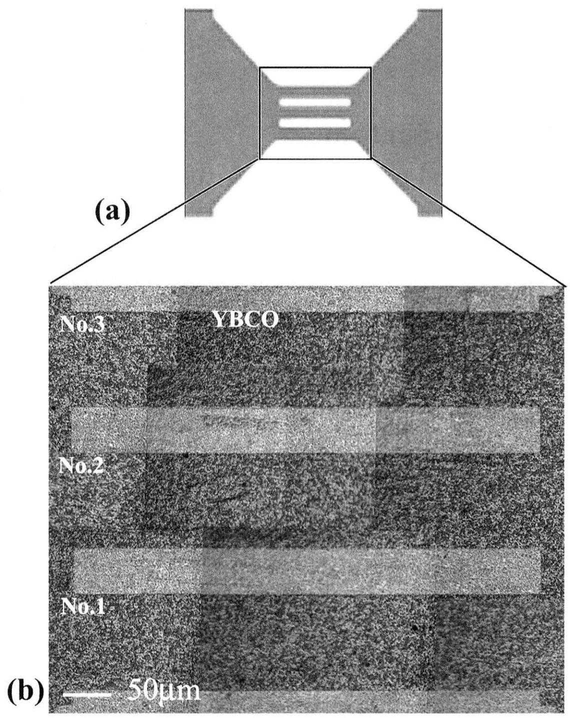

Fig. 3　**(a)** Pattern of multi-filaments and **(b)** Optical micrograph of multi-filaments area in YBCO tape.

voltage response, δV which is synchronized with the laser modulation frequency, f_{mod} will be observed. The intensity of signal (δV) in this hot-spot is proportionate to the local electric field, E [2].

Figure 2 shows the schematic diagram of the SSM system for current flow measurement. It is consisted of a dc SQUID magnetometer made of

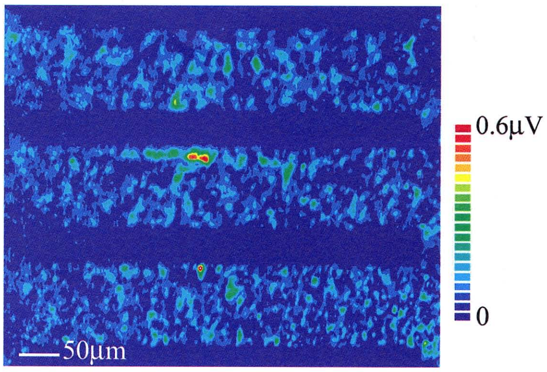

Fig. 4 Reconstruction of the CC microstructure from SE image.

Nb-based tunnel Josephson junction and a pick-up coil of 10μm in diameter. By performing a 2D scanning of the sample surface that is being biased with a dc applied current, we are able to detect its local magnetic flux by the pick-up coil as a function of position. The magnetic flux corresponds to the perpendicular component of the self magnetic-field of the multi-filament. The 2D local current distribution was then constructed from the self-field image by using the inverted Biot-Savart's law [8].

3. Experimental

The HTS CC used in this experiment is a $CVD-YBCO/PLD-CeO_2/IBAD-GZO/Hastelloy$. It has 0.5$\mu$m thick YBCO layer and I_c of 156A. A multi-filament structure as shown in **Fig. 3(a)** was formed in the YBCO CC using typical photolithography and wet etching process. The dimension of the multi-filament was a parallel of three-filament structure of 100μm wide by 500μm long with 50μm wide gaps in between. **Fig. 3(b)** represents its optical micrograph. The condition for the low temperature scanning at 88.7K is; laser power of 0.1mW, modulation frequency of 2.3kHz, stepping distance of 5μm with I_b of 12.4, 13.6 and 14.0mA.

Self magnetic-field data was measured using SSM at I_b of 10mA. In order to make estimation of J_c distribution, we combined the LTSLM data complementary with current density distribution obtained from the SSM. Ratio of the average I_c for each filament was estimated from the average local J_c distribution.

4. Results and Discussion

Figure 4 shows the SEI image of the CC multi-filaments visualizing defects. In general, the multi-filaments gave response of about 200nV that can be interpreted that the YBCO CC is made up of grains

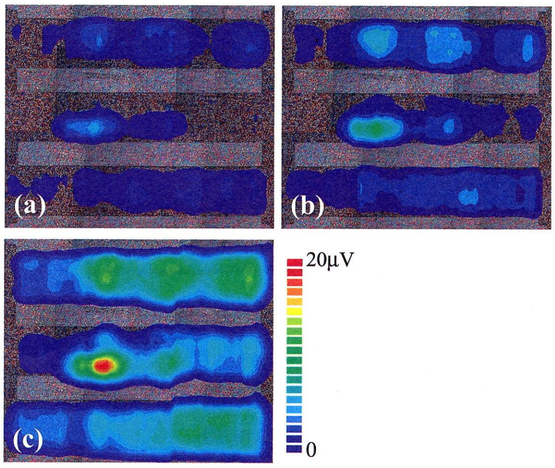

Fig. 5 LTSLM images of the flux flow dissipation that is superimposed on the optical micrograph of the filaments, obtained at 88.7K with I_b of **(a)** 12.4mA, **(b)** 13.6mA and **(c)** 14.0 mA.

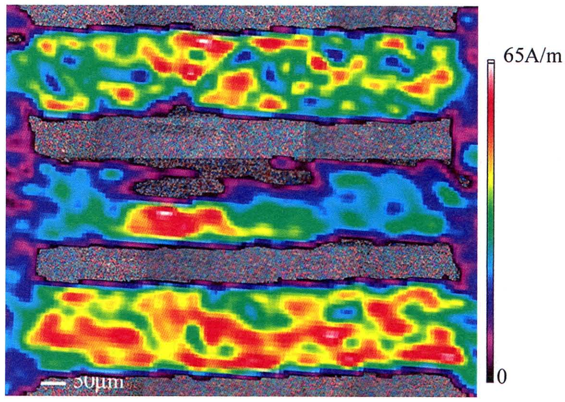

Fig. 6 Current density distribution estimated from SSM.

having good crystallinity. However, further inspection showed local defects were also present based on the higher SE voltage signals. We can identify localized defected locations at the upper part of the middle bridge. These defects acted as obstacles that will obscure the supercurrent flow.

The superconducting experiment was done at 88.7K by using the LTSLM. By applying the initial I_b in **Fig. 5(a)**, laser irradiation caused the 'weakest' section easily transit to a resistive state and $V > 0$ appears over it. At higher I_b, almost every cross section responsed to the laser irradiation but the defected areas such as bridge No.2 were more prone to the resistive transition as the bias current is increased. The dissipative area grew percolatively based on the interaction of the current flow to the presence of local defects.

Figure 6 shows the distribution of the local cur-

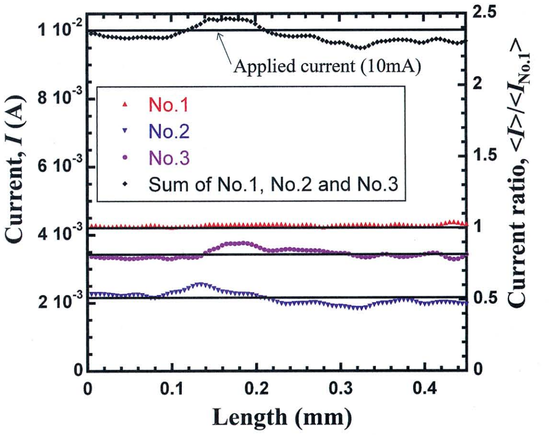

Fig. 7 Current distribution that was integrated from current density then plotted as a function of position along the length of each filaments.

rent flow that was measured using SSM. By converting self magnetic-field information, we obtained the local supercurrent flow in each filament[8]. We found that the supercurrent flowed inhomogeneously in each filament due to avoiding current limiting obstacles.

The filamentary structure allows the current to be shared and the total amount of the current flow depends on the current carrying capability of each filaments. By integrating the local current density along the width of each filament, we can validate that the current estimation for all three filaments hold because the total current agreed with the applied current value as in **Fig. 7**. Due to the dimension of the pattern we used, we obtained the highest current value for filament No.1 which has the shortest current pass from the current terminals. Due to the defected area in bridge No. 2, only half of the current amount can be passed through it. However, at I_b of 10mA, the integrated current verified that our current estimation by using SSM still hold.

The right hand side of y-axis in **Fig. 7** is the average current ratios of each filament to the current of filament No.1. We can see that for filament No. 2, due to the influence of local obstacles, the amount of current passing through it has a ratio of 0.51 while filament No. 3 has a ratio of 0.82. In an ideal case, the ratio of current flowing in each filament should be one.

5. Local J_c Estimation

Combining the independent information of the local current density distribution with the information of local flux flow dissipation from LTSLM al-

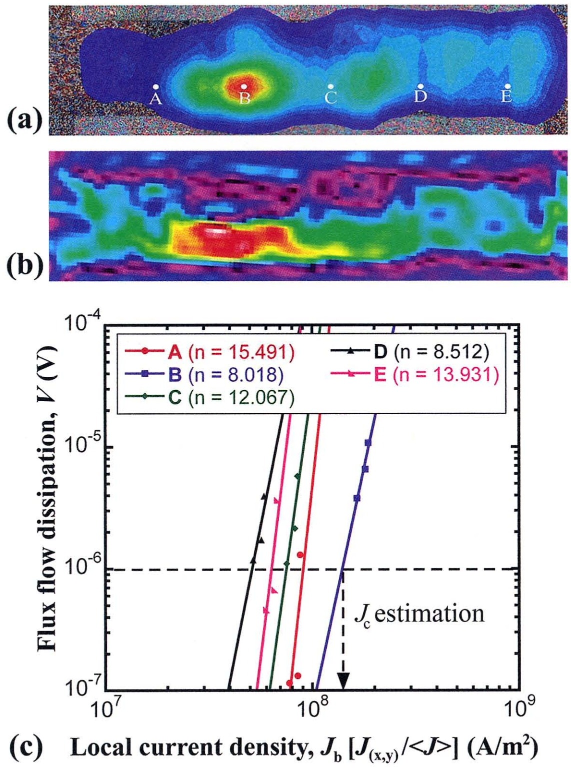

Fig. 8 (**a**) Super-impose of flux flow dissipation with optical micrograph of filament No. 2. Points A-E are the position for local $V-J$ estimation, (**b**) Current density distribution and (**c**) Local $V-J$ characteristics based on LTSLM and SSM information.

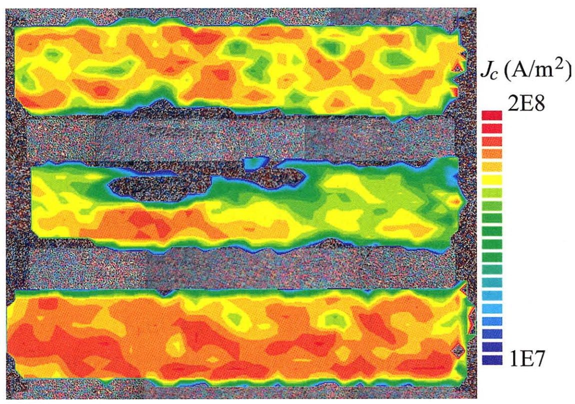

Fig. 9 Local J_c estimation.

lowed us to estimate the actual local J_c distribution and I_c in each filament.

We first investigate its local $V-J$ characteristics to estimate its local J_c by setting its voltage threshold, V_c. At selected spots in **Fig. 8(a)**, the local $V-J$ characteristics are estimated by plotting its local flux flow signals against the applied current weighted by the normalized current distribution obtained from SSM at each spot in **Fig. 8(b)**. The

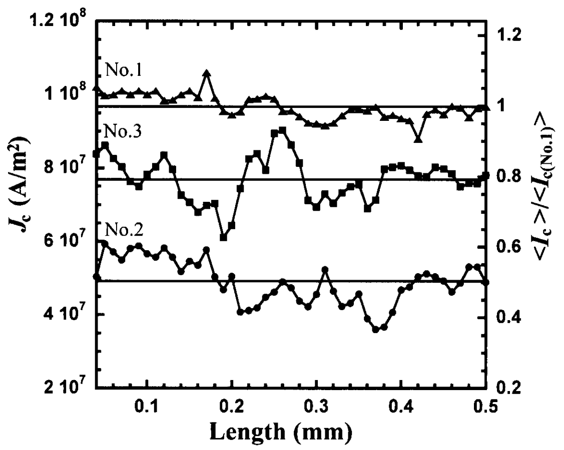

Fig. 10 Longitudinal distribution of integrated local J_c along the width for No.1, No.2 and No.3 as a function of position. The right y-axis correspond to the average I_c over average I_c of No. 1 based from the average local J_c value.

points are fitted using a power fitting curve and extrapolated. The J_c values can be estimated at the extrapolated J value using a critical voltage criterion of 1μV (the dotted line on the graph) in **Fig. 8(c)**.

By combining the matrix of the flux flow dissipation for all applied bias currents with its local current density distribution matrix, the resulting local J_c map can be seen as in **Fig. 9**; superimposed with its optical micrograph. From the local J_c map, we can see that the current sharing mechanism of the filaments depended on the microstructure of the filaments. The local obstacles on filament No.2 made an absence of current flow. If we calculate I_c values in each filament by integrating local J_c across the width as shown in **Fig. 10**, the I_c ratio shows good agreement with that of transport current in **Fig. 7**. This indicates that the I_c ratio in each filament controls the current flow in the filaments.

6. Conclusion

Local current flow and dissipation in a three parallel 100μm-wide filamentary YBCO tapes have been studied. By using the novel method of J_c and I_c estimations, we have shown that the present methods allowed us to estimate critical currents in each filament with a resolution of several μm scale. We also have measured the current imbalance on the current sharing in the filamentary structure. It has been shown that the filaments' I_c is influenced significantly if the filament size reaches 100μm scale because of current blocking obstacles. Filament width as well as the properties and dimension of the stabilization layer should be designed taking into account such localized dissipation.

Present study also allows us to investigate underlying defects by combining site-specified TEM observation since we can find the location of the current blocking defects with good resolution. Related results will be published separately.

7. Acknowledgements

This work was partly supported by the New Energy and Industrial Technology Development Organization (NEDO) as Collaborative Research and Development of Fundamental Technologies for Superconductivity Applications and also supported by JSPS: KAKENHI (15360153).

References

1) W.J. Carr and C.E. Oberly, *IEEE Trans. Appl. Supercond.*, **9** pp. 1475-1478, 1999.
2) T. Kiss, M. Inoue, M. Yasunaga, H. Tokutomi, Y. Iijima, K. Kakimoto, T. Saitoh, Y. Tokunaga, T. Izumi and Y. Shiohara, *IEEE Trans. Appl. Supercond.*, **15** pp. 3656-3659, 2005.
3) D. Abraimov, D. M. Feldmann, A. A. Polyanskii, A. Gurevich, G. Daniels, D. C. Larbalestier, A. P. Zhuravel and A. V. Ustinov, *Appl. Phys. Lett* , **85** pp. 2568-2570, 2004.
4) D.M. Feldmann, J.L. Reeves, A.A. Polyanskii, A. Goyal, R. Feenstra, D.F. Lee, M. Paranthaman, D.M. Kroeger, D.K. Christen, S.E. Babcock and D.C. Larbalestier, *IEEE Trans. Appl. Supercond*, **11** pp. 3772, 2001.
5) G. Grimaldi, M. Bauer, H. Kinder, W. Prusseit, U. Gambardella and S. Pace, *Physica C*, **372-376** pp. 1009, 2002.
6) R. Gross and D. Koelle, *Rep. Prog. Phys*, **57** pp. 651, 1994.
7) Z. Zulkifli, T. Fujiwara, T. Shoyama, D. Mitsui, T. Kiss, K. Enpuku, K. Ohmatsu and Y.Shiohara, *Research Reports on Information Science and Electrical Engineering of Kyushu University*, **11** pp. 91-95, 2006.
8) K. Koyanagi, T. Kiss, M. Inoue, T. Nakamura, K. Imamura, M. Takeo and Y. Shiohara, *Physica C*, **445-448** pp. 677-681, 2006.